Monte Carlo simulation of diffusion of interacting electrons in lateral surface superlattices

Toshishige Yamada and D. K. Ferry
Center for Solid State Electronics Research, Arizona State University, Tempe, Arizona 85287-6206
(Received 23 April 1993)

We have studied the temperature dependence of the transport properties of two-dimensional (2D) electrons in a periodic potential, when the electrons interact through an interparticle Coulomb force. This many-body problem is solved numerically, with a molecular-dynamics Monte Carlo technique. The diffusion constant D shows a monotonic increase with temperature T, but the functional dependence is a power-law type $D \sim T^n$ rather than a simple activation type. This power-law dependence is due to the effect of the 2D potential giving rise to a spatial transition of an electron from a potential minimum to another equivalent potential minimum, together with an interparticle Coulomb interaction causing friction in the electron motion and hence forming a dressed electron. The result is fit to the previous theory in the context of a particle moving in a periodic potential with a friction force, and the exponent K in the power-law expression shows a consistent potential dependence with the model.

I. INTRODUCTION

Two-dimensional (2D) electrons in a superlattice potential, with a potential period $a \sim 0.1$ μm, can now be realized experimentally in a lateral surface superlattice embedded in a field-effect transistor (FET) structure with a mesh-gate electrode.[1,2] The 2D superlattice potential can be represented by the summation of two cosine functions, $V(x,y)=V_0[\cos(2\pi x/a)+\cos(2\pi y/a)+2]/4$ with a peak-to-peak amplitude V_0. If the electron characteristic energy E is larger than the saddle-point energy $V_0/2$ of the 2D potential, they are free to move except for those regions where the 2D potential energy is larger than E and an antidote array is formed. On the contrary, if $E < V_0/2$, electrons are mainly confined in the 2D potential minima and a quantum dot array is formed. The interparticle Coulomb interaction is known to play an essential role in the context of Coulomb blockade in small structures coupled with barriers, through which the electrons tunnel.[3] In the present situation of electrons in a 2D periodic potential, the Coulomb interaction has a significant influence on electron transport if the electron areal density is small ($\sim 10^{10}$ cm^{-2}) so that the interparticle Coulomb interaction will not be well screened.[4] A noninteracting, independent electron picture with the Fermi energy as the characteristic electron energy is no longer adequate. The motion of a particular electron affects that of other electrons and there is nonlinear feedback to the original electron. The electrons do not populate the bottom of the 2D potential and are driven apart some reasonable distance to reduce the interparticle Coulomb energy, which increases the average potential energy of these electrons. It has been shown[4] that the velocity autocorrelation does not show a simple exponential decay but a damped oscillation, whose frequency is identified as that of the 2D plasma oscillation for small V_0. The Coulomb interaction also gives a considerable contribution to the diffusivity.

In this paper, we study the temperature dependence of the transport properties of interacting electrons by calculation of the diffusivity using a molecular-dynamics Monte Carlo technique.[4] Without the interparticle Coulomb interaction, the diffusion constant D will just show an activated temperature dependence[5] as $D \sim \exp(-\alpha/k_B T)$ due to the 2D potential, where an activation energy α can be related to the barrier height, k_B is the Boltzmann constant, and T is the temperature. Only when having enough energy to overcome the potential barrier, an electron can contribute to the diffusion and such probability is given by this formula. In the presence of the interparticle Coulomb interaction, however, the temperature dependence changes drastically. When one electron moves from one local potential minimum to another local potential minimum, the movement of the electron gives a perturbation to the neighboring electrons and they move in a manner correlated with the first electron: the electron is dressed by the other electrons and the transition probability from one potential minimum to another has to be renormalized. This problem has been studied by Kondo[6] in the context of the diffusion of an atom in a metal, where the atom interacts with conduction electrons through a Coulomb interaction. The important conclusion is that the transition matrix element Δ from one potential minimum to another is renormalized by a factor $(k_B T/W)^K$ due to the Coulomb interaction, where W is the bandwidth of the electrons and K is the coupling constant. The diffusion constant D is then given by the squared matrix element $\Delta^2(k_B T/W)^{2K}$ divided by the broadening of the electron energy level T, resulting in $D \sim T^{2K-1}$. This result is independent of the detail of the transition mechanism and the interaction (the expressions of K and W are model dependent), and is applicable to other systems like ours, if there is a mechanism for a particle to move from one site to another equivalent site, and there is an interaction between the particle and the surrounding environment so that the particle is "dressed" by this interaction.[6,7] In the present model, the transition of a particle between multiple equivalent sites is provided by the 2D potential, where an electron tends to move from one potential

0163-1829/93/48(11)/8076(7)/$06.00

minimum to another, and the interaction with the surrounding environment is provided by the interparticle Coulomb interaction.

We have observed a power-law dependence of the diffusion constant D in our simulation results. The exponent $2K-1$ is positive for all the potential amplitudes $V_0=2.5-20$ meV studied here, and D is a monotone increasing function of temperature. The interparticle Coulomb interaction increases with V_0 due to the reduction of interparticle distance, and the exponent K indicating the interaction strength also increases with V_0, and this is consistent with Kondo's theory. The result is further compared to the theoretical model in the context of a particle moving in a periodic potential proposed by Weiss and Grabert,[8] and the observed exponent K in the power law shows a consistent potential dependence with the model. In Sec. II, the model and the numerical techniques are explained, and in Sec. III, the results and discussion are given. Our conclusions are given in Sec. IV.

II. SIMULATION MODEL

Electrons are treated as particles, rather than quantum-mechanical wave packets, moving in a 2D potential created in a gated GaAs structure $V(x,y)=V_0[\cos(2\pi x/a)+\cos(2\pi y/a)+2]/4$ with a potential period $a=0.16$ μm. (The dimensions were taken from the experiments of Ref. 1.) The electron areal density is assumed to be 1.4×10^{10} cm^{-2} (on average, only 3.6 electrons per unit cell), for which the Fermi energy is 0.39 meV and we assume a parabolic band. We consider electron transport for $4.2<T<50$ K, where the thermal energy is larger than this Fermi energy and the classical statistics prevail.[9] In this situation, it has been shown that the interparticle Coulomb interaction dominates electron dynamics, due to the weak screening of the Coulomb potential because of the small number of electrons per unit cell, and scattering by phonons and impurities gives only a small perturbation to the system.[4] In fact, the velocity autocorrelation function shows a damped oscillation, whose frequency is identified as that of the 2D plasma oscillation for small V_0, and the Coulomb interaction gives a significant contribution to the diffusion.

The interparticle Coulomb interaction is treated with a molecular-dynamics technique.[4,10,11] At each time step, a Coulomb force is calculated for all pairs of electrons and is used to update the position and the momentum of each electron during the subsequent time step. In this way, we include various many-body effects automatically without artificial assumptions for the screening or collective excitations.[12] We simulate 32 electrons in 3×3 unit cells, corresponding to the electron areal density 1.4×10^{10} cm^{-2} mentioned above, and a periodic boundary condition is imposed for this simulation square, with side length $L=3a$, to eliminate unwanted boundary effects. When an electron leaves the square by crossing the boundary $x=L$, another electron is input from the equivalent boundary $x=0$ with the same y coordinate, momentum, and energy. The number of electrons in the square remains constant throughout the simulation.

The Coulomb interaction has to be consistently defined within the periodic boundary condition. The most appropriate formulation of the Coulomb interaction, consistent with the periodic boundary condition, is related to the Ewald sum method and a minimum image approximation.[4,10,11] An electron is assumed to interact with the other $N-1$ electrons in the $L\times L$ simulation square through minimum image vectors. The minimum image vector $\mathbf{r}_{ij}$ connecting electrons i and j is defined as $\mathbf{r}_{ij}=\mathbf{x}_j-\mathbf{x}_i-n_x\mathbf{a}_x-n_y\mathbf{a}_y$, where $\mathbf{a}_x=(L,0)$ and $\mathbf{a}_y=(0,L)$, and n_x and n_y are chosen to be the integers to minimize the magnitude $|\mathbf{r}_{ij}|$. The Coulomb energy E_{Coul} for electron j used for the evaluation of the force is defined by the summation of the interparticle Coulomb energy within the minimum image approximation by

$$E_{\text{Coul}}=\frac{e^2}{4\pi\varepsilon}\sum_{i\neq j}\frac{1}{r_{ij}}\ , \tag{1}$$

where e is the unit charge, ε is the dielectric constant, r_{ij} is the length of the minimum image vector for electrons i and j, and the summation is taken over all the other $N-1$ ensemble electrons in the simulation square except electron j itself. The background positive charge to neutralize the electron negative charges is irrelevant in molecular dynamics as long as it is uniformly, continuously distributed (jellium), and its contribution is not included in (1). In the presence of the jellium background charge, there are two more terms for the Coulomb energy, the negative energy between the electrons and the jellium background charge, and the positive energy of the jellium background charge itself. The absolute values of those energies per simulation square (3×3 unit cells) can be related to an ensemble average $\langle E_{\text{Coul}}\rangle$ and are on the order of $2N\times\langle E_{\text{Coul}}\rangle$ and $N\times\langle E_{\text{Coul}}\rangle$ ($\langle E_{\text{Coul}}\rangle\sim11.7$ meV for a uniform electron distribution as shown in the discussion of Fig. 4 in Sec. III), respectively, and they are unchanged for different electron distributions by their definitions. Therefore, they do not contribute to the interparticle Coulomb force in molecular dynamics. Although they are important for the evaluation of the internal energy for the system, they just shift the energy origin and are not included in (1).

Once the force acting on a particle is well defined, it is straightforward to solve Newton's equations numerically. We update the position x and the momentum p with a predictor-corrector method by[4,10]

$$x(i+1)=x(i)+p(i)\Delta t+f[x(i)](\Delta t)^2/2\ , \tag{2}$$

$$p(i+1)=p(i)+\{f[x(i)]+f[x(i+1)]\}\Delta t/2\ , \tag{3}$$

where $x(i)$ and $p(i)$ indicate the functional values of $x(t)$ and $p(t)$ at the ith time step of period Δt, and f is the summation of the interparticle Coulomb force and the 2D potential force (in the units of $m=1$). This algorithm is second-order accurate with respect to Δt and is quite stable. In fact, the elimination of the momentum terms from (2) and (3) results in Verlet's algorithm[13] which is known to be second-order accurate and also quite stable. With the use of double precision variables to minimize round-off errors, and with the choice of $\Delta t=10^{-17}$ s to

maintain high accuracy, excellent numerical energy conservation with an error as small as 0.01% is realized in the electron dynamics during a typical simulation for $\sim 10^2$ ps.

Although the interparticle Coulomb interaction is essential, realistic impurity[14] and phonon[15] scattering is included for completeness as usual with the ensemble Monte Carlo method. These occur as discrete events, where the former scattering is much more frequent at the low temperatures considered here. With the assumption of $\sim 10^{10}$ cm^{-2} interface impurities, the impurity-scattering limited mobility reaches 1.3×10^5 cm^2/V s at 4.2 K. Electrons perform a free flight between scattering events, under the influence of the force caused by the interparticle Coulomb potential and the 2D potential. If scattering occurs, electrons suddenly change their momentum (and energy in inelastic processes) and then start another free flight. We have adopted an envelope function[16] corresponding to the lowest subband in an FET channel and evaluated the quasi-2D scattering rates[15] in the inversion channel.

Finding an initial condition is not trivial, because of the interparticle Coulomb interaction. If any electrons are unusually close to one another in the initial condition, the Coulomb energy will lead to a rapid rise in electron kinetic energy and will cause an artificial heating of the electron system. We perform a preliminary simulation, before running the "real" simulation, to find an appropriate initial condition, using a molecular-dynamics Monte Carlo code with a slight modification. This consists of adding a perturbation to scale the electron momentum by $(\langle E_{\rm kin}\rangle/k_BT)^{1/2}$ at every $\sim 10^2$ time steps so that the ensemble average of the electron kinetic energy $\langle E_{\rm kin}\rangle$ is reset to the thermal energy k_BT. Actually, the equipartition law in a 2D system requires that $\langle E_{\rm kin}\rangle = k_BT$ in thermal equilibrium and this treatment forces the system to satisfy this requirement. This preliminary simulation can start with any conditions but $\langle E_{\rm kin}\rangle$ is usually chosen much larger than k_BT. Typically within ~ 10 ps, $\langle E_{\rm kin}\rangle$ is smoothly reduced to k_BT and maintains that value. As $\langle E_{\rm kin}\rangle$ approaches k_BT, the scaling perturbation is gradually turned off since the scaling factor approaches unity. When average energies are essentially time independent, an appropriate initial condition is obtained, which is characterized by $\langle E_{\rm kin}\rangle = k_BT$. In this preliminary simulation, electrons have exchanged energies with a heat bath through the momentum scaling perturbation and also exchanged energies among themselves through interparticle Coulomb interaction, and then reached an equilibrium. In essence, this is quite similar to a simulated annealing[4] of the electron system to find the proper initial condition that is allowed by equilibrium statistical mechanics.

The "real" simulation is performed without any momentum scaling perturbation being necessary, and therefore the total energy of the entire system is practically fixed (negligible inelastic phonon scattering at the low temperatures here). Although the interaction with the heat bath is terminated, the electrons still continue to exchange energies among themselves through the interparticle Coulomb interaction. However, this Coulomb interaction does not change the equilibrium properties of the system as is obvious in our method to find an initial condition. In fact, the kinetic-energy distribution function $f(E_{\rm kin})$ of an electron is expected to be time independent and proportional to $\exp(-E_{\rm kin}/k_BT)$ in thermal equilibrium. This point is checked in our numerical simulations, as will be discussed in the next section.

The "real" simulation provides raw data consisting of the position and the momentum of each electron at every time step. Using these values, we can evaluate the velocity autocorrelation function $\langle v_x(i)v_x(0)\rangle$, the mean-square displacement $\langle \Delta x^2(i)\rangle$, and the radial distribution function $g(r)$, where $\langle\cdots\rangle$ indicates the ensemble average. We create an Einstein plot of the mean-square displacement and evaluate the diffusion constant D from its temporal gradient by

$$D=\frac{1}{2}\frac{d}{dt}\langle \Delta x^2(t)\rangle \ , \tag{4}$$

rather than using the Kubo-Greenwood formula to integrate the correlation function.[4,10]

III. RESULTS AND DISCUSSION

Before analysis of the diffusivity as a function of temperature, it is important to see what kind of thermal equilibrium is realized in the simulation. Figure 1 shows energy densities $\log[n_1(E_{\rm kin})]$, $\log[n_2(E_{\rm kin}+E_{\rm pot})]$, and $\log[n_3(E_{\rm kin}+E_{\rm pot}+E_{\rm Coul})]$ in arbitrary units as a function of energy for $V_0=5$ meV at (a) 5.9 K and (b) 40 K in thermal equilibrium. Here, $E_{\rm kin}$ is the kinetic energy of an electron, $E_{\rm pot}$ is the 2D potential energy at the electron site, and $E_{\rm Coul}$ is the Coulomb energy of the electron defined in Sec. II, within the minimum image approximation (without the compensation of positive background). These energy densities are histograms of the number of electrons for the specified energy, and are combined by obvious relations, which are

$$n_1(E_{\rm kin})=\sum_{E_{\rm pot}} n_2(E_{\rm kin}+E_{\rm pot}) \ , \tag{5}$$

$$n_2(E_{\rm kin}+E_{\rm pot})=\sum_{E_{\rm Coul}} n_3(E_{\rm kin}+E_{\rm pot}+E_{\rm Coul}) \ , \tag{6}$$

where the summations are taken over the ensemble electrons. They are calculated in the "real" simulation and show no time dependence. The energies $E_2=E_{\rm kin}+E_{\rm pot}$ or $E_3=E_{\rm kin}+E_{\rm pot}+E_{\rm Coul}$ are no longer a simple quadratic function of the momentum (also a function of the position) due to the 2D potential and the interparticle Coulomb interaction. Then, the corresponding state density $\rho_2(E_2)$ or $\rho_3(E_3)$ are not constant, and $n_2(E_2)$ and $n_3(E_3)$ are not proportional to the energy distribution function. However, $E_1=E_{\rm kin}$ *is* a quadratic function of momentum and the state density $\rho_1(E_1)$ is constant as usual in a 2D system. As shown in the figure, the energy density $\log[n_1(E_1)]$ can be well fit by a straight line defined by the thermal energy, and therefore the Maxwell distribution is empirically realized. The high-energy tails of $\log[n_2(E_2)]$ and $\log[n_3(E_3)]$ are almost the same as that of $\log[n_1(E_1)]$. The shapes of $n_2(E_2)$ and $n_3(E_3)$

are similar and this indicates that the Coulomb interaction basically gives an energy offset. Because of the interparticle Coulomb interaction included, electrons have to move away from the bottom of the potential well, which increases the ensemble average $\langle E_{\rm pot} \rangle$ and makes the state densities $\rho_2(E_2)$ and $\rho_3(E_3)$ small for small arguments of E_2 and E_3. This causes small energy densities $n_2(E_2)$ and $n_3(E_3)$ for small E_2 and E_3.

This can be also seen in the radial distribution function $g(r)$, which is shown in Fig. 2 for $T=5.9$ and 40 K. For clarity, the function for 40 K is offset by unity. In both cases, $g(r)$ is essentially zero for small r, rises at some r, and has a finite value around unity for larger r. The presence of the interparticle Coulomb interaction makes $g(r)$ practically zero for small r for the same reason as given above. At $T=5.9$ K, $g(r)$ shows an oscillation with the first peak around $r/L=0.13$, a little smaller than the interparticle distance of a uniform 2D electron gas $r/L=1/\sqrt{32}=0.17$ due to the effect of the 2D potential, and the second peak around $r/L=1/3$, corresponding to the 2D potential period. The first peak corresponds to a spatial order of electrons inside the unit cell and the second corresponds to a spatial order of electrons among the unit cells. At $T=40$ K, the oscillation in $g(r)$ practically disappears and $g(r)$ approaches that of a uniform 2D electron gas, which is $g(r)=1$, although $g(r)$ is still zero for small r.

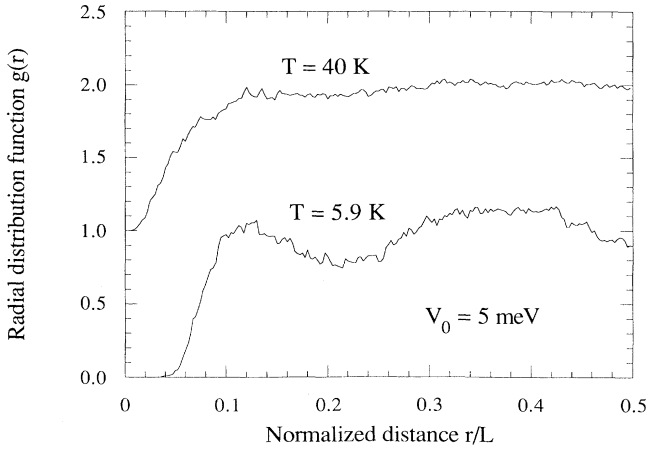

FIG. 2. Radial distribution function $g(r)$ as a function of normalized distance r/L at 5.9 and 40 K for $V_0=5$ meV.

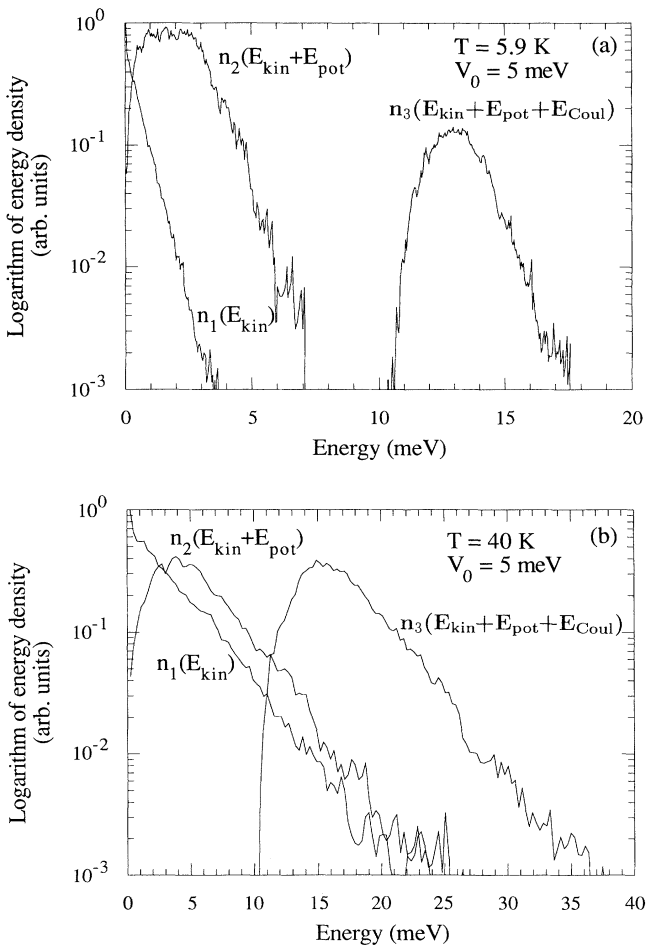

FIG. 1. Energy densities $\log[n_1(E_{\rm kin})]$, $\log[n_2(E_{\rm kin}+E_{\rm pot})]$, and $\log[n_3(E_{\rm kin}+E_{\rm pot}+E_{\rm Coul})]$ at (a) 5.9 K and (b) 40 K for $V_0=5$ meV.

Figure 3 shows the summation of ensemble averages $\langle E_{\rm kin} \rangle$ and $\langle E_{\rm pot} \rangle$ in thermal equilibrium as a function of temperature T from 4.2 to 50 K for various potential amplitudes $V_0=2.5$ (white circle), 5 (black circle), 10 (white square), 15 (black square), and 20 meV (white diamond). The apparent relation seen in the figure is that $\langle E_{\rm kin}+E_{\rm pot} \rangle$ increases with V_0 at any temperature. Since $\langle E_{\rm kin} \rangle$ is equal to the thermal energy $k_B T$, $\langle E_{\rm pot} \rangle$

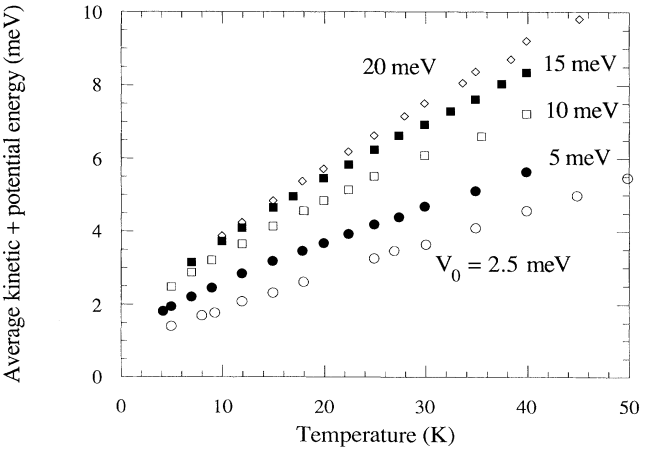

FIG. 3. Plot of $\langle E_{\rm kin}+E_{\rm pot} \rangle$ in thermal equilibrium as a function of temperature T from 4.2 to 50 K for various potential amplitudes $V_0=2.5$ (white circle), 5 (black circle), 10 (white square), 15 (black square), and 20 meV (white diamond).

is responsible for this increase with V_0. In fact, electrons always have to keep some reasonable separation to reduce the interparticle Coulomb energy and this causes the increase in $\langle E_{\rm pot} \rangle$ with V_0, although there is a slight change in the Coulomb energy itself with V_0, as will be seen below. The quantity $\langle E_{\rm kin}+E_{\rm pot} \rangle$ is a monotone function of T, but it is not a simple linear function over the temperature range. The nonlinearity is noticeable at low temperatures, especially for large V_0. At high temperatures, the characteristics can be fit by straight lines but each has a different gradient. Because of the interparticle Coulomb interaction, the curves will have a finite value of $\langle E_{\rm pot} \rangle$ even if they are extrapolated to $T=0$ as was discussed above. The saddle-point energy $E_{\rm sad}$ of the 2D potential is $V_0/2$ and it can be seen in the figure that $\langle E_{\rm kin}+E_{\rm pot} \rangle$ is larger than $E_{\rm sad}$ over the entire temperature range for $V_0=2.5$ meV, while $\langle E_{\rm kin}+E_{\rm pot} \rangle < E_{\rm sad}$ for $V_0=20$ meV. However, the Einstein plot of the mean-square displacement as a function of time shows a linear behavior in the long-time limit for both cases, and the diffusion constant is well defined for both. The change is continuous from nearly-free-electron transport ($V_0=2.5$ meV) to classical-hopping transport ($V_0=20$ meV) as V_0 increases, due to the smooth shape of the energy density $n_2(E_{\rm kin}+E_{\rm pot})$ at finite temperatures discussed above. No sharp, discontinuous transition from a mobile phase to an immobile phase is observed.

Figure 4 shows the ensemble average of the interparticle Coulomb energy per electron $\langle E_{\rm Coul} \rangle$ as a function of temperature for various potential amplitudes. Compared to the larger variation of $\langle E_{\rm kin}+E_{\rm pot} \rangle$ as a function of temperature in Fig. 3, $\langle E_{\rm Coul} \rangle$ shows a much smaller change. The Coulomb energy increases with potential amplitude V_0 at any temperature. This is due to the decreasing interparticle distance as V_0 is increased. In the high-temperature limit, all the curves converge to one energy value, which is the Coulomb energy of a spatially uniform 2D electron gas. The Coulomb energy is an increasing function of temperature for a small potential amplitude, such as $V_0=2.5$ meV, and is a decreasing function for a large potential amplitude, such as $V_0=20$ meV. The 2D potential with small V_0 helps electrons align in an orderly manner with a reasonable interparticle distance, and this reduces the Coulomb energy compared to that of a uniform 2D electron gas. However, the 2D potential with large V_0 acts to reduce the interparticle distance, which increases the Coulomb energy instead.

The diffusion constant D is readily evaluated by producing an Einstein plot of the mean-square displacement as a function of time. The phonon scattering is infrequent in the temperature range considered here (4.2–50 K). The electron dynamics within classical statistics are dominated by the Coulomb interaction and the 2D periodic potential, with a small perturbation from impurity scattering (and negligible phonon scattering).[4] Figure 5(a) shows a logarithmic plot of the diffusion constant as

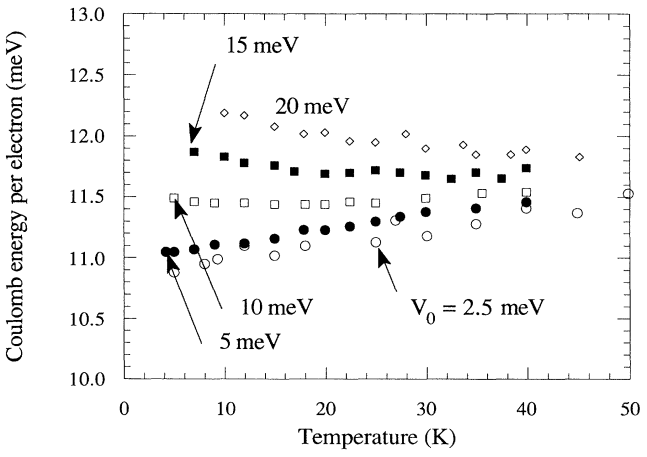

FIG. 4. Plot of interparticle Coulomb energy per electron $\langle E_{\rm Coul} \rangle$ as a function of temperature T from 4.2 to 50 K for various potential amplitudes $V_0=2.5$ (white circle), 5 (black circle), 10 (white square), 15 (black square), and 20 meV (white diamond).

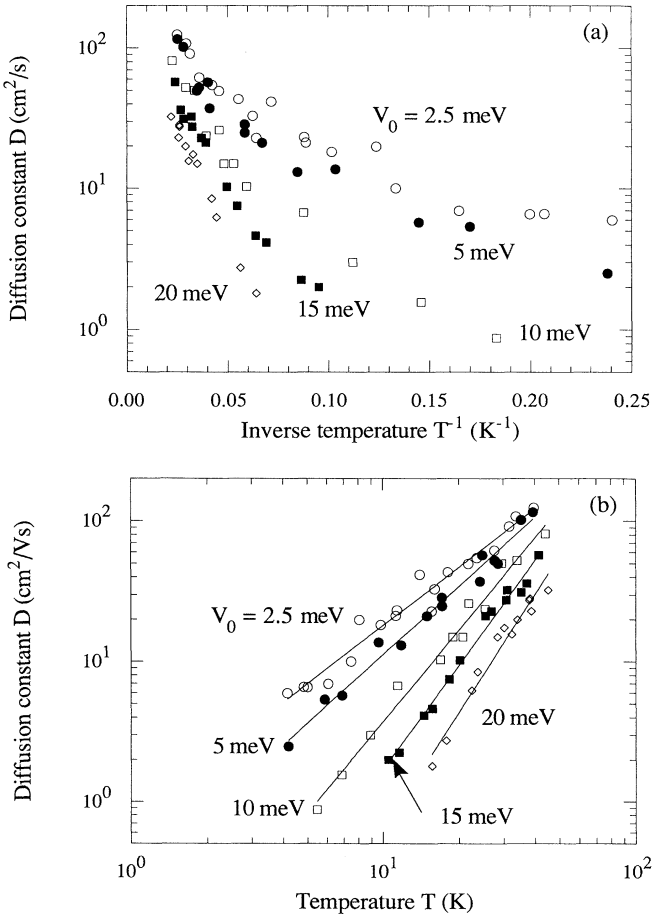

FIG. 5. Diffusion constant D as a function of temperature T from 4.2 to 50 K for various potential amplitudes $V_0=2.5$ (white circle), 5 (black circle), 10 (white square), 15 (black square), and 20 meV (white diamond): (a) $\log[D\ (\rm cm^2/s)]$ as a function of T^{-1} ($\rm K^{-1}$), and (b) $\log[D\ \rm cm^2/s)]$ as a function of $\log[T\ (\rm K)]$.

a function of the inverse temperature for various potential amplitudes. If the diffusion is well described by the activation law $D \sim \exp(-\alpha/k_B T)$, then the results should be fit to straight lines. However, data points seem to form a downward convex curve for each V_0, where the second derivative of the curve $d^2 \log D/d(T^{-1})^2$ is not zero but a finite positive value. This suggests that the activation law does not apply to the present situation and another physical picture has to be sought. Figure 5(b), on the other hand, shows a log-log plot of the diffusion constant as a function of temperature, where each line is a straight-line fit. The diffusivity can be best described by a power law $D \sim T^n$, rather than the activation law by comparison of Figs. 5(a) and 5(b). This power-law dependence is not surprising but is expected to be commonly observed in a system with an interparticle interaction that causes friction to the particle motion. According to Kondo,[6] the transition matrix element Δ corresponding to the probability of a particle moving from one site to another equivalent site is dressed by the (interparticle) interaction to give $\Delta(T/W)^K$, where W is the bandwidth of the electrons and K is the coupling of the interaction. The diffusion constant D is given the squared matrix element $\sim T^{2K}$ divided by the effective level broadening T, resulting in $D \sim T^{2K-1}$. The assumption made in the derivation of this theory is $k_B T \gg 2\pi\hbar\Delta$,[6] where $\hbar$ is Planck's constant, and this will be shown to be satisfied later. This result of the power-law relation is quite universal and does not depend on the detail of the physical transition mechanism (tunneling or excitation, etc.) nor the detail of the interaction (Coulomb interaction or electron-phonon interaction, etc.),[7] although the expressions for K and W are model dependent. In the present model, the 2D periodic potential gives rise to Δ, and the interparticle Coulomb interaction is responsible for the renormalization of Δ by $\Delta(T/W)^K$. The coupling K has a monotone increasing dependence on V_0, as shown in the figure. In fact, as shown in Fig. 4, the interparticle Coulomb energy increases with V_0, and therefore causes larger coupling K.

A theory more specific to the present model was developed in the context of electrons in a periodic potential well by Weiss and Grabert,[8] although they assume tunneling for the transition mechanism and an electron-phonon interaction for the friction mechanism. The tunneling is characterized by a transition matrix element Δ and the electron-phonon interaction is characterized by a friction force $\eta\, dx/dt$ appearing in a Newton's equation, with η being the friction coefficient. Because of the friction, Δ is renormalized and is given by $\Delta(\pi k_B T/\hbar\omega_0)^K$, where $K=\eta a^2/2\pi\hbar$ and a is the potential period. The frequency ω_0 is defined by the curvature of the potential well by $V''(x_0)=m\omega_0^2$, where x_0 is the bottom of the potential well. The diffusion constant D is then given by[8]

$$D=2\pi^{1/2}\frac{\Delta^2}{\omega_0}\frac{\Gamma(K)}{\Gamma(K+\frac{1}{2})}(\pi k_B T/\hbar\omega_0)^{2K-1}, \tag{7}$$

where Γ indicates the gamma function. From our simulation result, we can estimate K and evaluate the magnitude of the undressed transition matrix element Δ.[17] This is summarized in Table I. The second column $\hbar\omega_0$ is determined from the curvature of the potential $V''(x)$ and the third column K is obtained from our simulation result in Fig. 5(b). The fourth column of undressed matrix element Δ is calculated by using (7), with D values evaluated in Fig. 5(b). The undressed matrix element Δ should be constant if the theory applies to the present model, and we can observe that this is the case here: the undressed matrix element is $\Delta=(1.5-1.7)\times 10^{11}$ s^{-1}. The dilute bounce gas approximation[8] was assumed to derive (7), which can be stated by a condition $(\Delta/\omega_0)^2 \ll 1$ when $K>1$. As is seen in Table I, $(\Delta/\omega_0)^2 < 10^{-2}$ and this condition is satisfied. The theory considers a tunneling for a transition mechanism of an electron from cell to cell and the applicability of the theory is limited to the temperature range of $k_B T < \hbar\omega_0$.[8] We do not have this restriction since the present transition is not due to tunneling but to the excitation by the other electrons through the interparticle Coulomb interaction, and the power law works beyond that temperature in our simulation. It should also be noted that the assumption made in the derivation of Kondo's theory requires $k_B T \gg 2\pi\hbar\Delta$, and this is satisfied in the temperature range here, as can be seen in Table I.

If we examine the experimental possibility to observe the predicted power-law dependence, we notice that the discrete nature of the dopants would give an amplitude fluctuation to the periodic potential assumed here and in the Weiss and Grabert's theory, and as a result, the perfect periodicity of the potential might be lost. However, the perfect periodicity is not an essential requirement for the power-law dependence of the diffusion constant: Kondo's theory in Refs. 6 and 7 considers a hopping or tunneling of a particle from one potential minimum to another potential minimum, and no spatial order of these sites is assumed. Thus, the power-law dependence is still expected in the presence of this fluctuation, but the expression (7) may have to be modified accordingly. The study of such potential fluctuation effects is left to a future work.

TABLE I. Fitting to the power-law relation.

V_0 (meV)	ω_0 (10^{12}/s)	$\hbar\omega_0$ (K)	observed K	observed Δ (10^{11}/s)
2.5	2.31	17.6	1.19	1.5
5	3.27	24.9	1.31	1.7
10	4.63	35.2	1.59	1.7
15	5.66	43.1	1.69	1.7
20	6.56	49.9	1.89	1.5

IV. CONCLUSION

The temperature dependence of the transport property of 2D electrons in a 2D periodic potential with an interparticle Coulomb interaction has been studied by molecular-dynamics Monte Carlo technique. The diffusion constant D shows a monotonic increase with temperature but the functional dependence is not a simple activation type $D \sim \exp(-\alpha/k_B T)$. The study shows that the curve is best fit by a power law $D \sim T^{2K-1}$. This power-law dependence is due to the effect of a spatial transition of an electron from a potential minimum to another equivalent potential minimum, together with an interparticle Coulomb interaction causing a friction to the electron motion and hence forming a dressed electron. It is observed that the interparticle Coulomb energy increases with the 2D potential amplitude V_0 due to the reduction of the interparticle distance, and the exponent K indicating the interaction strength increases with V_0, which is consistent with Kondo's theory. The result is further fit to a model by Weiss and Grabert in the context of a particle moving in a periodic potential, and the exponent K in the power-law expression shows a consistent potential dependence with the model.

ACKNOWLEDGMENTS

This work has been supported by the Office of Naval Research.

[1]J. Ma, R. A. Puechner, W.-P. Liu, A. M. Kriman, G. N. Maracas, and D. K. Ferry, Surf. Sci. **229**, 341 (1990); E. Paris, J. Ma, A. M. Kriman, D. K. Ferry, and E. Barbier, J. Phys. Condens. Matter **3**, 6605 (1991); D. K. Ferry, Prog. Quantum Electron. **16**, 251 (1992), and references therein.

[2]See, for example, *Granular Nanoelectronics,* edited by D. K. Ferry, J. R. Barker, and C. Jacoboni (Plenum, New York, 1990); *Nanostructure and Mesoscopic Systems,* edited by W. P. Kirk and M. A. Reed (Academic, San Diego, 1991); C. W. J. Beenakker and H. van Houten, in *Solid State Physics,* edited by H. Ehrenreich and D. Turnbull (Academic, San Diego, 1991), Vol. 44.

[3]K. K. Likharev, IBM J. Res. Dev. **32**, 144 (1988); D. V. Averin and K. K. Likharev, in *Mesoscopic Phenomena in Solids,* edited by B. L. Al'tshuler, P. A. Lee, and R. A. Webb (Elsevier, Amsterdam, 1991).

[4]T. Yamada and D. K. Ferry, Phys. Rev. B **47**, 1444 (1993); **47**, 6416 (1993).

[5]C. Kittel, *Introduction to Solid State Physics,* 6th ed. (Wiley, New York, 1986).

[6]J. Kondo, Physica B **84**, 40 (1976).

[7]J. Kondo and T. Soda, J. Low Temp. Phys. **50**, 21 (1983); J. Kondo, Physica B **126**, 377 (1984).

[8]U. Weiss and H. Grabert, Phys. Lett. **108A**, 63 (1985).

[9]One might assume that the effect of antisymmetrization of the entire electron wave function is relevant in the present context and the exchange modifications should be included within molecular dynamics. This has actually been done by A. M. Kriman, M. J. Kann, D. K. Ferry, and R. P. Joshi, Phys. Rev. Lett. **64**, 1619 (1990), by inclusion of an exchange interaction in the molecular dynamics based on the Hartree-Fock scheme using a wave-packet wave function for the description of an individual wave function, and the method was applied to a two-dimensional electron system by R. P. Joshi, A. M. Kriman, M. J. Kann, and D. K. Ferry, Appl. Phys. Lett. **58**, 2369 (1991). The latter paper has shown that the exchange interaction is relevant only for higher electron areal densities ($\sim 10^{12}$ cm^{-2}) and plays essentially no role for the small density ($\sim 10^{10}$ cm^{-2}) considered here.

[10]M. P. Allen and D. J. Tildesley, *Computer Simulation of Solid* (Clarendon, Oxford, 1987).

[11]P. Lugli and D. K. Ferry, Appl. Phys. Lett. **46**, 594 (1985); Phys. Rev. Lett. **56**, 1295 (1986); D. K. Ferry, *Semiconductors* (Macmillan, New York, 1991); D. J. Adams and G. S. Dubey, J. Comput. Phys. **72**, 156 (1987).

[12]The molecular dynamics treats the electron-electron interaction as a continuous event realized in the electron motion under the influence of the interparticle Coulomb force. If we include the electron-electron interaction as a discrete event with the Born approximation or its modifications and treat the interaction as an instantaneous scattering event to change the momentum in the free flight of an electron, then the long-range nature of the Coulomb interaction cannot be expressed properly. The best way to see this is to check how a plasma oscillation, representing the nature of the dielectric function in the limit $q \rightarrow 0$, is realized in the simulation. In the discrete event picture with the Born approximation or its modifications, each electron moves independently between scattering events, and the correlation of the electron motion—the motion of one electron affects that of the other electrons and also gives feedback to the original one—cannot be expressed properly. The velocity autocorrelation function always shows a simple exponential decay with time, and the plasma oscillation cannot be observed. On the other hand, in molecular dynamics, this correlation can be automatically included in the electron dynamics without artificial assumptions. Actually, we have observed the plasma oscillation in the time evolution of the velocity autocorrelation function and recovered the correct plasma frequency as a function of the electron density as reported in Ref. 4. This indicates the significant advantage of the molecular dynamics over the Born approximations and its modifications.

[13]L. Verlet, Phys. Rev. **159**, 98 (1967); **165**, 201 (1968).

[14]F. Stern and W. E. Howard, Phys. Rev. **163**, 816 (1967).

[15]P. J. Price, Ann. Phys. (N.Y.) **133**, 217 (1981).

[16]F. F. Fang and W. E. Howard, Phys. Rev. Lett. **16**, 797 (1966); F. Stern, Phys. Rev. B **5**, 4891 (1972); T. Ando, A. B. Fowler, and F. Stern, Rev. Mod. Phys. **54**, 437 (1982).

[17]The definition of the matrix element Δ basically follows that of Ref. 6 (although the author defines $h\Delta$ as the matrix element) and twice of that of Ref. 8.,